ACS APPLIED MATERIALS & INTERFACES

Research Article

www.acsami.org

Effects of Immersion Solvent on Photovoltaic and Photophysical Properties of Porphyrin-Sensitized Solar Cells

Hironobu Hayashi,[‖] Tomohiro Higashino,[‖] Yuriko Kinjo,[‖] Yamato Fujimori,[‖] Kei Kurotobi,[†] Pavel Chabera,[§] Villy Sundström,[*,§] Seiji Isoda,[†] and Hiroshi Imahori[*,‖,†]

[‖]Department of Molecular Engineering, Graduate School of Engineering and [†]Institute for Integrated Cell-Material Sciences (WPI-iCeMS), Kyoto University, Nishikyo-ku, Kyoto 615-8510, Japan

[§]Department of Chemical Physics, Lund University, Box 124, 22100 Lund, Sweden

Supporting Information

ABSTRACT: Memory effects in self-assembled monolayers (SAMs) of zinc porphyrin carboxylic acid on TiO_2 electrodes have been demonstrated for the first time by evaluating the photovoltaic and electron transfer properties of porphyrin-sensitized solar cells prepared by using different immersion solvents sequentially. The structure of the SAM of the porphyrin on the TiO_2 was maintained even after treating the porphyrin monolayer with different neat immersion solvents (memory effect), whereas it was altered by treatment with solutions containing different porphyrins (inverse memory effect). Infrared spectroscopy shows that the porphyrins in the SAM on the TiO_2 could be exchanged with the same or analogous porphyrin, leading to a change in the structure of the porphyrin SAM. The memory and inverse memory effects are well correlated with a change in porphyrin geometry, mainly the tilt angle of the porphyrin along the long molecular axis from the surface normal on the TiO_2, as well as with kinetics of electron transfer between the porphyrin and TiO_2. Such a new structure–function relationship for DSSCs will be very useful for the rational design and optimization of photoelectrochemical and photovoltaic properties of molecular assemblies on semiconductor surfaces.

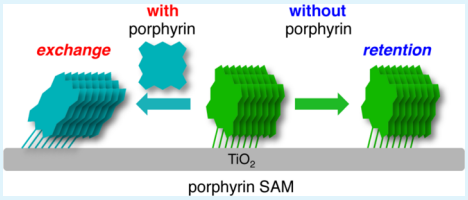

KEYWORDS: *porphyrin, dye-sensitized solar cell, self-assembled monolayer, titanium oxide, memory effect*

INTRODUCTION

Elucidating the structural details of molecular assemblies formed on surfaces is essential in understanding a variety of fundamental surface and interface phenomena as well as developing new types of functional surfaces and interfaces. Examples include molecular electronic devices[1−3] and adsorption of biological molecules and materials.[4−6] In the past the vast majority of such studies have been performed for thiol-based self-assembled monolayers (SAMs) which can be formed on gold surfaces by immersion.[7,8] In contrast, the use of thiol-based SAMs on other metal and semiconducting surfaces has been limited technologically.[9,10] Meanwhile, carboxylic and phosphonic acids have been frequently employed as an anchoring group for the immobilization of functional molecules on semiconducting surfaces.[1,11,12] However, their studies have focused mainly on function rather than structure. As such, adsorption/desorption and exchange behavior of functional molecules on semiconducting surfaces and their structure–function relationship have not been fully addressed.

As a promising alternative to silicon-based solar cells, considerable efforts have been devoted to the development of dye-sensitized solar cells (DSSCs) where a SAM of dye is formed on a highly porous semiconducting electrode.[13−21] In particular, porphyrin-sensitized solar cells (PSSCs)[22−65] have drawn much attention in DSSCs because of the potential advantage of porphyrins over ruthenium dyes in terms of cost, molecular design, and light-harvesting properties. On the basis of a push–pull concept as well as asymmetrical π-elongation, cell performances of PSSCs have been improved rapidly. In particular, push–pull porphyrins have been developed intensively in recent years with the aim of better matching between the absorption and solar spectra, reaching a power conversion efficiency (η) of more than 10%.[53,59−65] To achieve further improvement of the cell performances, it is also important to elucidate a close relationship between the dye structure, film structure, and photophysics and photovoltaic properties, providing a guideline for the rational molecular design of high-performance dyes.

We have extensively examined the effects of substituents and adsorption conditions on the photovoltaic and photophysical properties of PSSCs.[41,66,67] From these results we have demonstrated that the porphyrin geometry on the TiO_2 electrode controls through-space electron transfer (ET) kinetics on the TiO_2.[66,67] Namely, more upright geometry of the zinc porphyrin (ZnP) on the TiO_2 slows down electron injection from the porphyrin excited singlet state (^{1}ZnP*) to a conduction band (CB) of the TiO_2 as well as charge recombination (CR) from the electron in the CB of the

Received: June 11, 2015
Accepted: August 4, 2015
Published: August 12, 2015

DOI: 10.1021/acsami.5b05163
ACS Appl. Mater. Interfaces 2015, 7, 18689−18696

TiO_2 to the porphyrin radical cation ($ZnP^{\bullet+}$), leading to improvement in the short circuit current (J_{SC}) and resulting η-values. In particular, the η-value of PSSC prepared by the treatment of a TiO_2 electrode with a MeOH immersion solution of the porphyrin is significantly higher than that prepared by the treatment of a TiO_2 electrode with the corresponding *tert*-butyl alcohol:acetonitrile mixture (v/v = 1:1) (denoted as *t*-BuOH:MeCN) (vide infra). These results imply that immersion solvents influence the structure of porphyrin SAMs, mainly the tilt angle (θ) of the porphyrin along the long molecular axis from the surface normal on TiO_2 surfaces greatly.

During the course of our studies, we accidently encountered "memory effects" of the photovoltaic properties in the porphyrin SAMs on the TiO_2 that could be regulated by choice of the immersion solvents (MeOH vs *t*-BuOH/MeCN) with and without the porphyrins. Although there are some examples of memory effects of SAMs induced by external stimuli,[68−70] "memory effects" of photovoltaic properties by SAMs have not been reported in organic photovoltaics devices. Herein we report the first example of the memory effects in porphyrin SAMs on TiO_2 electrodes that can be controlled by immersion solvents, which have been evaluated by the photovoltaic properties of PSSCs, complemented by measurements of electron transfer kinetics and SAM composition and thickness. CN-labeled ZnP carboxylic acid (CNMP)[67] and the reference porphyrin (MP)[41,66,67] were used in this study (Figure 1).

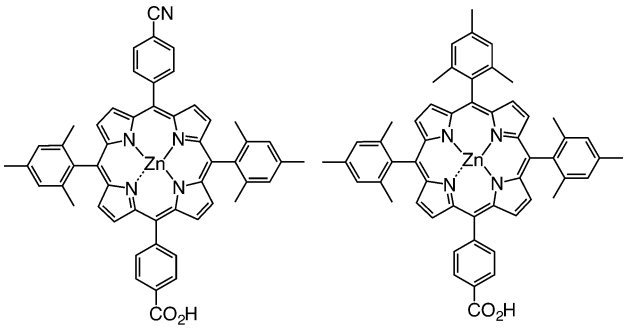

Figure 1. Molecular structures of porphyrin sensitizers.

EXPERIMENTAL SECTION

Instruments. UV−visible absorption spectra were obtained on a PerkinElmer Lambda 900UV/vis/NIR spectrometer. Attenuated total reflectance-Fourier transform infrared (ATR-FTIR) spectra were taken with the Smart iTR diamond anvil ATR accessory (NICOLET 6700, Thermo scientific), using typically 512 scans at a resolution of 4 cm^{-1}. All samples were placed in contact with the diamond window using the same mechanical force. Photocurrent−voltage characteristics were measured by PECK2400-N with PEC-L11 solar simulator (Peccell Technologies) under standard two-electrode conditions (100 mW cm^{-2}, AM1.5). Photocurrent action spectra were recorded with CEP-2000RR (BUNKOUKEIKI). TEM micrographs were measured by applying a drop of the sample to a carbon-coated copper grid. Images were recorded using a JEM-2200FS transmission electron microscope (JEOL).

Materials. All solvents and chemicals were of reagent-grade quality, purchased commercially, and used without further purification unless otherwise noted. The synthesis and characterization of [5-(4-carboxyphenyl)-15-(4-cyanophenyl)-10,20-bis(2,4,6-trimethylphenyl)-porphyrinato]zinc(II) (CNMP)[67] and [5-(4-carboxyphenyl)-10,15,20-tris(2,4,6-trimethylphenyl)porphyrinato]zinc(II) (MP)[41] were reported previously.

Sample Preparation of Porphyrin-Sensitized TiO_2 Films. Nanoporous films were prepared from a colloidal suspension of TiO_2 nanoparticles (P25, Nippon Aerogel) dispersed in distilled water.[41] This TiO_2 colloidal suspension was deposited on a transparent conducting glass substrate (Asahi Glass, SnO_2: F, 8 ohm/sq) by using the doctor blade technique. The films were annealed for 10 min at 673 K for the 4-μm-thick TiO_2 films, followed by similar deposition and annealing (723 K, 2 h) for the 10-μm-thick TiO_2 films. The thickness of the films was determined using a surface roughness tester (SURFCOM 130A, ACCRETECH). First, the TiO_2 electrodes were sensitized in a 0.2 mM porphyrin solution of *t*-BuOH:MeCN or MeOH at room temperature (step I). Then, after washing the TiO_2 electrodes were further immersed into *t*-BuOH/MeCN or MeOH with and without 0.2 mM porphyrin at room temperature (step II). After removal from the porphyrin bath, the nonadsorbed molecules were washed off by rinsing the films with the same solvent, and the films were dried at room temperature for ∼20 s to yield the porphyrin-sensitized TiO_2 films.

Photovoltaic Measurements. The photovoltaic measurements were performed in a sandwich cell consisting of the dye-sensitized electrode as the working electrode and a platinum-coated glass electrode as the counter electrode.[41] The two electrodes were placed on top of each other using a thin transparent Surlyn polymer film (Dupont) as a spacer for the electrolyte solution (0.5 M LiI, 0.01 M I_2, 0.6 M dimethylpropyl imidazolium iodide, and 0.5 M 4-*tert*-butylpyridine in MeCN). The IPCE and current−voltage characteristics were determined by a PEC-L 11 solar simulator (Peccell, Japan) irradiated with simulated air mass (AM) 1.5 solar light (100 mW cm^{-2}). All experimental values were given as an average of five independent measurements.

Transient Absorption (TA) Spectroscopy. The femtosecond laser setup is based on a MaiTai seeded Spitfire Pro XP amplifier (Spectra Physics) with central output wavelength of 796 nm and 1 kHz repetition rate delivering ∼60 fs pulses.[66,67] The beam was split into two parts: one for pumping a collinear optical parametric amplifier (TOPAS-C, Light Conversion) to generate the pump beam (555 nm), while the second part was led through a computer-controlled delay line and used to generate the probe beam in a second TOPAS-C parametric amplifier (665 nm). Subsequently, the probe pulses were split into two parts: one overlapping with the pump pulse in the sample volume and another serving as a reference. The probe and the reference beams were then detected with photodiode (PD) detectors (Pascher Instruments). The intensity of excitation pulses was kept below 5×10^{14} photons·$pulse^{-1}$·cm^{-2}. Absorption spectra were measured before and after experiments to check for possible sample degradation, and films were moved during the experiments to prevent photo and thermal damage. The mutual polarization between pump and probe beams was set to the magic angle (54.7°) by placing Berek compensator in the pump beam. The porphyrin-sensitized TiO_2 films for the TA spectroscopy measurement were prepared by a similar procedure as described above for the photovoltaic measurements. A parafilm spacer of ∼100 μm was placed on top of the TiO_2/porphyrin film, and the cell was closed by a thin glass slide, while the volume between the slides was filled with acetonitrile. Binder clips were used to press the glass assembly to prevent solvent evaporation during measurements (Figure S1). Multiexponential fitting of measured kinetics was performed in Matlab software.

RESULTS AND DISCUSSION

Photovoltaic Properties. To evaluate the memory effects of immersion solvent on the photovoltaic properties of the CNMP-sensitized solar cell, we used the stepwise procedure (steps I, II) for preparing the porphyrin-stained TiO_2 electrodes with two different immersion solvents, yielding contrasting photovoltaic performances.[41] Namely, the TiO_2 electrodes were initially immersed into either *t*-BuOH/MeCN or MeOH with 0.2 mM porphyrin at room temperature (step I). Then, after

DOI: 10.1021/acsami.5b05163
ACS Appl. Mater. Interfaces 2015, 7, 18689−18696

Table 1. Device Characteristics of Solar Cells under AM1.5 Conditions (100 mW cm^{-2})

	step I			step II							
entry	dye	solvent[a]	time/h[b]	dye	solvent[a]	time/h[b]	J_{sc}/[c] mA cm^{-2}	V_{oc}/[c] V	ff[c]	η/[c] %	θ/[d] deg
1	CNMP	*t*-BuOH/MeCN	1				4.9 ± 0.1	0.64 ± 0.01	0.68 ± 0.01	2.1 ± 0.1	63 ± 2[f]
2	CNMP	*t*-BuOH/MeCN	1	CNMP	MeOH	12	6.1 ± 0.1	0.70 ± 0.01	0.68 ± 0.01	2.9 ± 0.1	52 ± 7
3	CNMP	*t*-BuOH/MeCN	1		MeOH	12	4.6 ± 0.1	0.62 ± 0.01	0.70 ± 0.01	2.0 ± 0.1	64 ± 7
4	CNMP	*t*-BuOH/MeCN	1		*t*-BuOH/MeCN	12	4.6 ± 0.1	0.66 ± 0.01	0.69 ± 0.01	2.1 ± 0.1	–
5	CNMP	MeOH	1				7.3 ± 0.2	0.69 ± 0.01	0.67 ± 0.02	3.4 ± 0.2	42 ± 4
6	CNMP	MeOH	1	CNMP	*t*-BuOH/MeCN	12	5.4 ± 0.2	0.69 ± 0.01	0.66 ± 0.02	2.5 ± 0.2	62 ± 8
7	CNMP	MeOH	1		*t*-BuOH/MeCN	12	7.1 ± 0.2	0.71 ± 0.01	0.67 ± 0.02	3.4 ± 0.2	39 ± 4
8	CNMP	MeOH	1		MeOH	12	6.8 ± 0.2	0.72 ± 0.01	0.68 ± 0.02	3.4 ± 0.2	–
9[e]	MP	*t*-BuOH/MeCN	1				7.6 ± 0.2	0.69 ± 0.02	0.64 ± 0.02	3.4 ± 0.3	53 ± 7[f]
10[e]	MP	MeOH	1				9.4 ± 0.2	0.76 ± 0.02	0.64 ± 0.01	4.6 ± 0.1	

[a]Immersion solvent. [b]Immersion time. [c]Average values from five independent experiments. [d]Tilt angle determined by TEM measurements. [e]Taken from ref 41. [f]Taken from ref 67.

washing the TiO_2 electrodes were further immersed into *t*-BuOH/MeCN or MeOH with and without 0.2 mM porphyrin at room temperature (step II). Finally, the porphyrin-stained electrodes were rinsed repeatedly with the same solvent as for the adsorption. Current–voltage characteristics and photocurrent action spectra were measured using the 10-μm-thick TiO_2 electrode stained with CNMP and a Pt counter electrode under standard AM 1.5 conditions.[41] The detailed adsorption procedures (steps I, II) and their photovoltaic properties under the different adsorption conditions (entries 1–10) are listed in Table 1.

For instance, when the TiO_2 electrode was sensitized solely by immersing it into *t*-BuOH/MeCN containing 0.2 mM CNMP in 1 h, the η-value of PSSC was found to be 2.1% (entry 1), as shown in Figure 2 and Table 1. Unexpectedly, when the TiO_2 electrode was sensitized under the same condition for step I, followed by washing and immersing into MeOH containing 0.2 mM CNMP in 12 h (step II), the η-value of PSSC was increased remarkably to 2.9% (entry 2). After treatment under the same condition for step I, additional treatment only in MeOH in 12 h (entry 3) or *t*-BuOH/MeCN in 12 h (entry 4) yielded no effect on the photovoltaic properties. Opposite stepwise sensitization experiments were also performed. When the TiO_2 electrode was sensitized solely by immersing it into MeOH containing 0.2 mM CNMP in 1 h, the η-value of PSSC reached 3.4% (entry 5), which is close to the η-value (2.9%) of PSSC under the entry 2 condition. Contrary, when the TiO_2 electrode was sensitized under the same condition for step I, followed by washing and immersing into *t*-BuOH/MeCN containing 0.2 mM CNMP for 12 h (step II), the η-value of PSSC was decreased remarkably to 2.5% (entry 6), which is close to the η-value (2.1%) of PSSC under the entry 1 condition. After treatment under the same condition for step I, additional treatment only in *t*-BuOH/MeCN in 12 h (entry 7) or MeOH in 12 h (entry 8) gave no effect on the photovoltaic properties. Note that the porphyrin molecules are densely packed on the TiO_2, showing formation of the porphyrin SAM on the TiO_2 ($(1.1–1.3) \times 10^{-10}$ mol cm^{-2})[41] and no significant desorption of the porphyrin immobilized on the TiO_2 occurred under the step II procedure (entries 3 and 7). These results imply that (i) once the porphyrin SAM is formed on the TiO_2, the structure of porphyrin SAM on the TiO_2 is retained even after treating the porphyrin SAMs with different neat immersion solvents (memory effect) and (ii) the structure of the porphyrin SAM

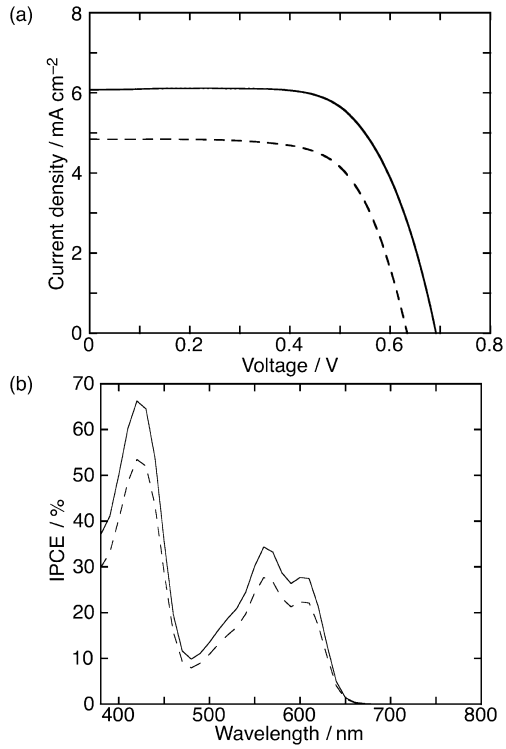

Figure 2. (a) Current density–voltage curves and (b) photocurrent action spectra of CNMP-sensitized solar cells (entry 1, dashed line; entry 2, solid line).

on the TiO_2 is altered solely by treatment with different immersion solutions with porphyrin (inverse memory effect). These results suggest that there is an equilibrium between the porphyrins in the SAM on TiO_2 and any exchangeable porphyrins in the immersion solution, and they are exchanged with time to reach the stable equilibrated state depending on the type of the porphyrin, concentration, immersion solvent, and temperature. During the exchanging process, there would be a transient void space at the exchanging site between the porphyrins. Therefore, the TiO_2 surface contacting directly the immersion solvent may be responsible for the change of porphyrin SAM on the TiO_2 surface. Namely, the structure of the porphyrin SAM, mainly the tilt angle of the porphyrin molecular axis on TiO_2, would be changed by a higher degree of freedom in the SAM structure.

DOI: 10.1021/acsami.5b05163
ACS Appl. Mater. Interfaces 2015, 7, 18689–18696

Characterization of Porphyrin SAMs. The porphyrin MP is known to have a similar dependence of the cell performance on the immersion solvent as CNMP (entries 9 and 10 in Table 1).[48] To confirm the above hypothesis, the TiO_2 electrode prepared in the CNMP/MeOH solution for 1 h (step I) was further immersed into a MP/MeOH solution (step II). ATR-FITR measurement on the TiO_2 electrode showed that the signal intensity of the CN group arising from CNMP at 2232 cm^{-1} decreases with increasing immersion time of step II, reaching the plateau in 4 h (Figures 3 and 4). Moreover, the

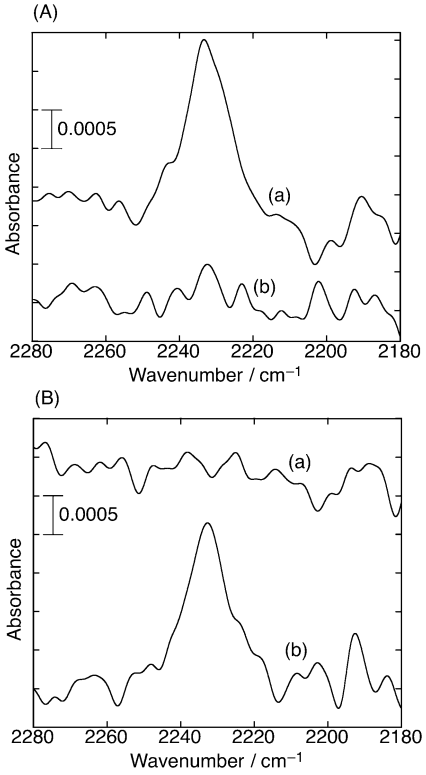

Figure 3. (A) ATR-FTIR spectra of the TiO_2 electrodes (a) prepared by immersing the MeOH solution containing CNMP in 1 h (step I) and (b) further immersed into the MeOH solution containing MP in 12 h (step II). (B) ATR-FTIR spectra of the TiO_2 electrodes (a) prepared by immersing the MeOH solution containing MP in 1 h (step I) and (b) further immersed into the MeOH solution containing CNMP in 12 h (step II).

opposite behavior was observed when the MP/MeOH TiO_2 electrode (1 h immersion) was further treated with a CNMP/MeOH solution, i.e., an increase in the CN intensity with increasing immersion time of step II. During these experiments there was no change in the porphyrin visible absorption spectra (Figure 5). These results unambiguously show that exchange of the porphyrin molecules in the SAM on the TiO_2 is essential to change in the SAM structure, resulting in further alternation in the cell performances.

We have already reported that the θ value of the porphyrin on TiO_2 determines the porphyrin core-TiO_2 ET distance and electron injection and CR between the porphyrin and TiO_2 occurs through space, rather than through the bridge connecting the porphyrin to the TiO_2 surface.[66,67] A simple linear correlation between the θ value and the concentration of long-lived electrons in the conduction band of TiO_2 was shown to exist. Namely, the more perpendicular orientation of the

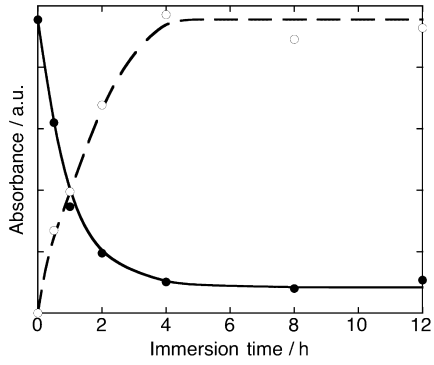

Figure 4. Change in IR signal intensity of the CN group at 2232 cm^{-1} as a function of immersion time of step II (solid line with black circles: The TiO_2 electrode, prepared by immersing the MeOH solution containing CNMP in 1 h (step I), was further immersed into the MeOH solution containing MP (step II); dashed line with white circles: The TiO_2 electrode, prepared by immersing the MeOH solution containing MP in 1 h (step I), was further immersed into the MeOH solution containing CNMP (step II)).

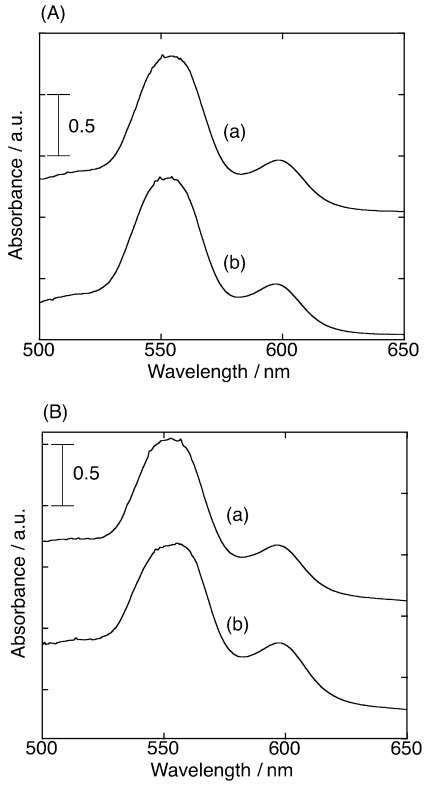

Figure 5. (A) UV−vis absorption spectra of the TiO_2 electrodes (a) prepared by immersing the MeOH solution containing CNMP in 1 h (step I) and (b) further immersed into the MeOH solution containing MP in 12 h (step II). (B) UV−vis absorption spectra of the TiO_2 electrodes (a) prepared by immersing the MeOH solution containing MP in 1 h (step I) and (b) further immersed into the MeOH solution containing CNMP in 12 h (step II).

adsorbed ZnP relative to the TiO_2 surface, the higher concentration of long-lived electrons in the CB, which contributes to the increase of photocurrent and η-value under the operating solar cell device. Transmission electron microscopy (TEM) measurements on TiO_2 nanoparticles sensitized under the different sensitization conditions provide support for the change in the tilted binding geometry of the

DOI: 10.1021/acsami.5b05163
ACS Appl. Mater. Interfaces 2015, 7, 18689−18696

porphyrin on TiO_2. For instance, the TEM of the sample prepared under the entry 2 condition reveal ca. 20 nm-sized TiO_2 nanoparticles covered with a thin porphyrin layer with an average thickness of 1.2 ± 0.1 nm, which is thicker than that of 0.9 ± 0.1 nm obtained under the entry 3 condition (Figure 6).

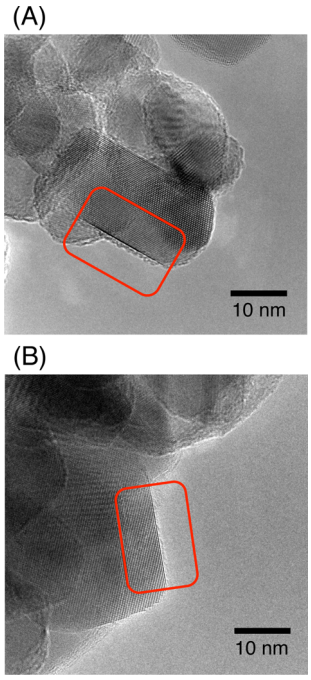

Figure 6. Typical TEM images of TiO_2 nanoparticles sensitized with (A) CNMP in *t*-BuOH:MeCN for 1 h, followed by treatment with CNMP in MeOH for 12 h (entry 2) and (B) CNMP in *t*-BuOH:MeCN for 1 h, followed by treatment without CNMP in MeOH for 12 h (entry 3). The average thicknesses of the porphyrin layers were determined as (A) 1.2 ± 0.1 nm and (B) 0.9 ± 0.1 nm.

Considering that the molecular length of CNMP along the long axis is 2.0 nm, the average tilt angles (θ) of the molecular axis with respect to the surface normal are estimated as 52 ± 7° for entry 2 and 64 ± 7° for entry 3 (Table 1). This agrees with the prediction that the porphyrin SAM on TiO_2 prepared initially with the mixed sensitization solvent would adopt more perpendicular geometry only after being sensitized with MeOH containing the same porphyrin molecules. The tilt angle of CNMP for entry 2 is smaller than those for entries 1 (θ = 63 ± 2°)[67] and 3. On the other hand, the tilt angle of CNMP for entry 6 (θ = 62 ± 8°) is larger than those for entries 5 (θ = 42 ± 4°) and 7 (θ = 39 ± 4°), which is in good agreement with the prediction that the porphyrin SAM on TiO_2 prepared initially with the MeOH sensitization solvent would adopt more tilted geometry only after being sensitized with the mixed solvent containing the same porphyrin molecules.

Transient Absorption Measurement. To obtain further insight about the behavior of porphyrin SAMs, we examined the photophysics of the ZnP-sensitized TiO_2 films by time-resolved TA spectroscopy. The interpretation of measured TA spectra has been discussed in detail in refs 66 and 67. Figure 7 displays TA kinetics at 665 nm since the differential TA spectrum at 665 nm has contributions from the oxidized dye.[66,67] The decay of the traces reflects the CR process and can be described by several components, ranging from subnanoseconds to more than several tens of nanoseconds (>50 ns). On the basis of the model of the CR process

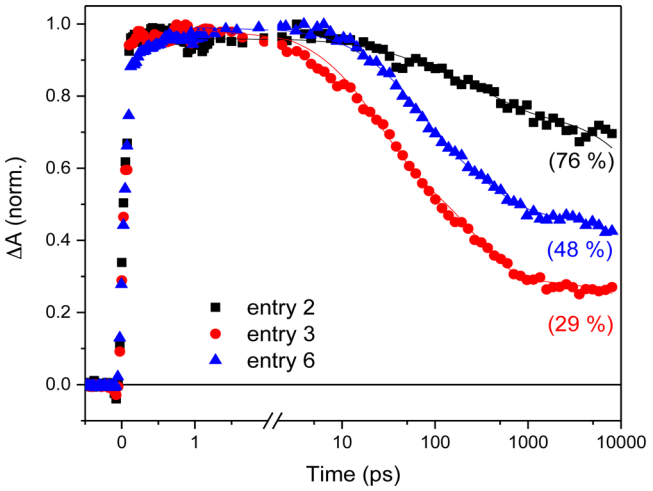

Figure 7. TA kinetics of CNMP on TiO_2 sensitized under different conditions (see Table 1 for details). The amplitudes of >50 ns component are shown in parentheses.

proposed previously,[66,67] the kinetics profiles were fitted (Figure 7). Note that the amplitude of the >50 ns recombination kinetic component (denoted as $A_{>50\ ns}$), corresponding to $ZnP^{\bullet+}$ that is quenched by the redox couple in the electrolyte solution, should correlate with the number of electrons collected in the external circuit per absorbed photon and thereby the J_{SC} and η-values in an operating DSSC.[66,67] In other words, the amplitude of long-lived component ($A_{>50\ ns}$) is directly related to the photovoltaic properties.

The amplitude of >50 ns component (76%) for the TiO_2 electrode first immersed into *t*-BuOH/MeCN and then followed by CNMP/MeOH treatment (entry 2) is significantly higher than that (29%) for the TiO_2 electrode prepared in the same manner but without CNMP present in the second sensitization step (entry 3). The amplitude of the slow, >50 ns, recombination phase of the electrode in entry 2 is almost as high as that of the electrode in entry 5 (single sensitization step in CNMP/MeOH, 1 h), which was shown to be close to 100% in our previous work.[67] The somewhat lower efficiency of the electrode in entry 2 (2.9%) as compared to that (3.4%) of the electrode in entry 5 agrees nicely with the somewhat lower amplitude (76%) of slow recombination compared to the almost 100% slow component of the electrode in entry 5.[67] This shows that the exchange of sensitizer molecules in the SAM layer is a slow (or a somewhat incomplete) process. These results also reveal that a nonoptimized electrode can be "repaired" by a second sensitization step in an optimized sensitizer/solvent combination (e.g., taking the step from electrode in entry 1 to entry 2).

Similarly, but perhaps of less practical interest, an optimized electrode can be "ruined" by a second sensitization step in a nonoptimized sensitizer/solvent combination. This is illustrated by comparing the electrodes in entry 5 (η = 3.4%; $A_{>50\ ns}$ = ~100%[67]) and entry 6 (η = 2.5%; $A_{>50\ ns}$ = 48% (Figure 7)). The second sensitization step in *t*-BuOH/MeCN brings the η-value and $A_{>50\ ns}$ down to 2.5% and 48%, respectively, close to the 2.0−2.1% efficiency and 29% of $A_{>50\ ns}$ for the electrodes in entries 1 and 3. That the lowest efficiency is not reached in the second sensitization step in the nonoptimal *t*-BuOH/MeCN solvent once more shows that the exchange process of the sensitizer molecules is incomplete over the time used in the present experiments. These changes of CR dynamics caused by

DOI: 10.1021/acsami.5b05163
ACS Appl. Mater. Interfaces 2015, 7, 18689−18696

a change of sensitization conditions all follow the trends expected from the above-discussed dependence on the sensitization procedure of the SAM structure and photovoltaic performance of the studied DSSCs.

CONCLUSION

In conclusion, we have successfully demonstrated memory effects of the photovoltaic properties of porphyrin SAMs on TiO_2 electrodes for the first time. The structure of the porphyrin SAM on the TiO_2 is retained after treating the porphyrin SAMs with different neat immersion solvents (memory effect), whereas it is changed by treatment with different immersion solutions containing a porphyrin (inverse memory effect). The porphyrin in the SAM on the TiO_2 is exchanged with the porphyrin in the immersion solution, leading to change in the structure of the porphyrin SAM. The memory and inverse memory effect correlate well with the change in the porphyrin binding geometry on TiO_2 as well as the electron transfer kinetics between the porphyrin and TiO_2. Although the involvement of immersion solvents for dye adsorption processes and their final structures on TiO_2 still remains elusive, the results obtained from porphyrin SAMs for DSSCs will be very informative for the rational design of molecular assemblies on semiconducting surfaces exhibiting excellent solar cell performances as well as photoelectrochemical and photovoltaic properties.

ASSOCIATED CONTENT

Supporting Information

The Supporting Information is available free of charge on the ACS Publications website at DOI: 10.1021/acsami.5b05163.

Sample assembly for TA measurements (Figure S1) (PDF)

AUTHOR INFORMATION

Corresponding Authors

*E-mail: imahori@scl.kyoto-u.ac.jp.

*E-mail: villy.sundstrom@chemphys.lu.se.

Notes

The authors declare no competing financial interest.

ACKNOWLEDGMENTS

This work was supported by Advanced Low Carbon Technology Research and Development Program (ALCA, JST), Grant-in-Aid (No. 25220801 to H.I.), and WPI Initiative, MEXT, Japan. The Swedish part of the work was supported by the Swedish Research Council (VR), the Knut and Alice Wallenberg Foundation, and the Swedish Energy Administration (STEM).

REFERENCES

(1) *Organic Electronics*; Klauk, H., Ed.; Wiley-VCH: Weinheim, 2006.

(2) Haran, A.; Waldeck, D. H.; Naaman, R.; Moons, E.; Cahn, D. The Dependence of Electron Transfer Efficiency on the Conformational Order in Organic Monolayers. *Science* **1994**, *263*, 948−950.

(3) Salomon, A.; Cahen, D.; Lindsey, S.; Tomfohr, J.; Engelkes, V. B.; Frisbie, C. D. Comparison of Electron Transport Measurements on Organic Molecules. *Adv. Mater.* **2003**, *15*, 1881−1890.

(4) Mrksich, M.; Whiteside, G. M. Using Self-Assembled Monolayers to Understand the Interactions of Man-Made Surfaces with Proteins and Cells. *Annu. Rev. Biophys. Biomol. Struct.* **1996**, *25*, 55−78.

(5) Whaley, S. R.; English, D. S.; Hu, E. L.; Barbara, P. F.; Belcher, A. M. Selection of Peptides with Semiconducting Binding Specificity for Directed Nanocrystal Assembly. *Nature* **2000**, *405*, 665−668.

(6) Kaganer, V. M.; Mohwald, H.; Dutta, P. Structure and Phase Transitions in Langmuir Monolayers. *Rev. Mod. Phys.* **1999**, *71*, 779−819.

(7) Ulman, A. *An Introduction to Ultrathin Organic Films: Langmuir-Blodgett to Self-Assembly*; Academic Press: New York, 1991.

(8) Love, J. C.; Estroff, L. A.; Kriebel, J. K.; Nuzzo, R. G.; Whitesides, G. M. Self-Assembled Monolayers of Thiolates on Metals as a Form of Nanotechnology. *Chem. Rev.* **2005**, *105*, 1103−1169.

(9) McGuiness, C. L.; Diehl, G. A.; Blasini, D.; Smilgies, D.-M.; Zhu, M.; Samarth, N.; Weidner, T.; Ballav, N.; Zharnikov, M.; Allara, D. L. Molecular Self-Assembly at Bare Semiconductor Surfaces: Cooperative Substrate−Molecule Effects in Octadecanethiolate Monolayer Assemblies on GaAs(111), (110), and (100). *ACS Nano* **2010**, *4*, 3447−3465.

(10) Alarcón, L. S.; Chen, L.; Esaulov, V. A.; Gayone, J. E.; Sánchez, E. A.; Grizzi, O. Thiol Terminated 1,4-Benzenedimethanethiol Self-Assembled Monolayers on Au(111) and InP(110) from Vapor Phase. *J. Phys. Chem. C* **2010**, *114*, 19993−19999.

(11) Lenz, T.; Schmaltz, T.; Novak, M.; Halik, M. Self-Assembled Monolayer Exchange Reactions as a Tool for Channel Interface Engineering in Low-Voltage Organic Thin-Film Transistors. *Langmuir* **2012**, *28*, 13900−13904.

(12) Kalyanasundaram, K.; Grätzel, M. Application of Functionalized Transition Metal Complexes in Photonic and Optoelectronic Devices. *Coord. Chem. Rev.* **1998**, *177*, 347−414.

(13) O'Regan, B.; Grätzel, M. A Low-Cost, High-Efficiency Solar Cell Based on Dye-Sensitized Colloidal TiO_2 Films. *Nature* **1991**, *353*, 737−740.

(14) Grätzel, M. Recent Advances in Sensitized Mesoscopic Solar Cells. *Acc. Chem. Res.* **2009**, *42*, 1788−1798.

(15) Nazeeruddin, M. K.; Angelis, F. D.; Fantacci, S.; Selloni, A.; Viscardi, G.; Liska, P.; Ito, S.; Bessho, T.; Grätzel, M. Combined Experimental and DFT-TDDFT Computational Study of Photoelectrochemical Cell Ruthenium Sensitizers. *J. Am. Chem. Soc.* **2005**, *127*, 16835−16847.

(16) Gao, F.; Wang, Y.; Shi, D.; Zhang, J.; Wang, M.; Jing, X.; Humphry-Baker, R.; Wang, P.; Zakeeruddin, S. M.; Grätzel, M. Enhance the Optical Absorptivity of Nanocrystalline TiO_2 Film with High Molar Extinction Coefficient Ruthenium Sensitizers for High Performance Dye-Sensitized Solar Cells. *J. Am. Chem. Soc.* **2008**, *130*, 10720−10728.

(17) Chen, C.-Y.; Wang, M.; Li, J.-Y.; Pootrakulchote, N.; Alibabaei, L.; Ngoc-le, C.; Decoppet, J.-D.; Tsai, J.-H.; Grätzel, C.; Wu, C.-G.; Zakeeruddin, S. M.; Grätzel, M. Highly Efficient Light-Harvesting Ruthenium Sensitizer for Thin-Film Dye-Sensitized Solar Cells. *ACS Nano* **2009**, *3*, 3103−3109.

(18) Han, L.; Islam, A.; Malapaka, C.; Chiranjeevi, B.; Zhang, S.; Yang, X.; Yanagida, M. High-Efficiency Dye-Sensitized Solar Cell with a Novel Co-Adsorbent. *Energy Environ. Sci.* **2012**, *5*, 6057−6060.

(19) Mishra, A.; Fischer, M. K. R.; Bäuerle, P. Metal-Free Organic Dyes for Dye-Sensitized Solar Cells: From Structure: Property Relationships to Design Rules. *Angew. Chem., Int. Ed.* **2009**, *48*, 2474−2499.

(20) Hagfeldt, A.; Boschloo, G.; Sun, L.; Kloo, L.; Pettersson, H. Dye-Sensitized Solar Cells. *Chem. Rev.* **2010**, *110*, 6595−6663.

(21) Clifford, J. N.; Martínez-Ferrero, E.; Viterisi, A.; Palomares, E. Sensitizer Molecular Structure-Device Efficiency Relationship in Dye Sensitized Solar Cells. *Chem. Soc. Rev.* **2011**, *40*, 1635−1646.

(22) Imahori, H.; Umeyama, T.; Ito, S. Large π-Aromatic Molecules as Potential Sensitizers for Highly Efficient Dye-Sensitized Solar Cells. *Acc. Chem. Res.* **2009**, *42*, 1809−1818.

(23) Martinez-Diaz, M. V.; de la Torre, G.; Torres, T. Lighting Porphyrins and Phthalocyanines for Molecular Photovoltaics. *Chem. Commun.* **2010**, *46*, 7090−7108.

DOI: 10.1021/acsami.5b05163
ACS Appl. Mater. Interfaces 2015, 7, 18689−18696

(24) Walter, M. G.; Rudine, A. B.; Wamser, C. C. Porphyrins and Phthalocyanines in Solar Photovoltaic Cells. *J. Porphyrins Phthalocyanines* **2010**, *14*, 759−792.
(25) Imahori, H.; Umeyama, T.; Kurotobi, K.; Takano, Y. Self-Assembling Porphyrins and Phthalocyanines for Photoinduced Charge Separation and Charge Transport. *Chem. Commun.* **2012**, *48*, 4032−4045.
(26) Li, L.-L.; Diau, E. W.-G. Porphyrin-Sensitized Solar Cells. *Chem. Soc. Rev.* **2013**, *42*, 291−304.
(27) Higashino, T.; Imahori, H. Porphyrins as Excellent Dyes for Dye-Sensitized Solar Cells: Recent Developments and Insights. *Dalton Trans.* **2015**, *44*, 448−463.
(28) Mozer, A. J.; Griffith, M. J.; Tsekouras, G.; Wagner, P.; Wallace, G. G.; Mori, S.; Sunahara, K.; Miyashita, M.; Earles, J. C.; Gordon, K. C.; Du, L.; Katoh, R.; Furube, A.; Officer, D. L. Zn-Zn Porphyrin Dimer-Sensitized Solar Cells: Toward 3-D Light Harvesting. *J. Am. Chem. Soc.* **2009**, *131*, 15621−15623.
(29) Ishida, M.; Park, S. W.; Hwang, D.; Koo, Y. B.; Sessler, J. L.; Kim, D. Y.; Kim, D. Donor-Substituted β-Functionalized Porphyrin Dyes on Hierarchically Structured Mesoporous TiO_2 Spheres. Highly Efficient Dye-Sensitized Solar Cells. *J. Phys. Chem. C* **2011**, *115*, 19343−19354.
(30) Kang, M. S.; Kang, S. H.; Kim, S. G.; Choi, I. T.; Ryu, J. H.; Ju, M. J.; Cho, D.; Lee, J. Y.; Kim, H. K. Novel D−π−A Structured Zn(II)-Porphyrin Dyes Containing a Bis(3,3-dimethylfluorenyl)amine Moiety for Dye-Sensitized Solar Cells. *Chem. Commun.* **2012**, *48*, 9349−9351.
(31) Liu, Y.; Lin, H.; Li, J.; Dy, J. T.; Tamaki, K.; Nakazaki, J.; Nakayama, D.; Nishiyama, C.; Uchida, S.; Kubo, T.; Segawa, H. Ethynly-Linked Push-Pull Porphyrin Hetero-Dimers for Near-IR Dye-Sensitized Solar Cells: Photovoltaic Performances versus Excited-State Dynamics. *Phys. Chem. Chem. Phys.* **2012**, *14*, 16703−16712.
(32) Odobel, F.; Blart, E.; Lagrée, M.; Villieras, M.; Boujtita, H.; El Murr, N.; Caramori, S.; Bignozzi, C. A. Porphyrin Dyes for TiO_2 Sensitization. *J. Mater. Chem.* **2003**, *13*, 502−510.
(33) Warnan, J.; Faverreau, L.; Meslin, F.; Severac, M.; Blart, E.; Pellegrin, Y.; Jacquemin, D.; Odobel, F. Diketopyrrolopyrrole−Porphyrin Conjugates as Broadly Absorbing Sensitizers for Dye-Sensitized Solar Cells. *ChemSusChem* **2012**, *5*, 1568−1577.
(34) Ball, J. M.; Davis, N. K. S.; Wilkinson, J. D.; Kirkpatrick, J.; Teuscher, J.; Gumming, R.; Anderson, H. L.; Snaith, H. J. A Panchromatic Anthracene-Fused Porphyrin Sensitizer for Dye-Sensitized Solar Cells. *RSC Adv.* **2012**, *2*, 6846−6853.
(35) Campbell, W. M.; Jolley, K. W.; Wagner, P.; Wagner, K.; Walsh, P. J.; Gordon, K. C.; Schmidt-Mende, L.; Nazeeruddin, Md. K.; Wang, Q.; Grätzel, M.; Officer, D. L. Highly Efficient Porphyrin Sensitizers for Dye-Sensitized Solar Cells. *J. Phys. Chem. C* **2007**, *111*, 11760−11762.
(36) Cherian, S.; Wamser, C. C. Adsorption and Photoactivity of Tetra(4-carboxyphenyl)porphyrin (TCPP) on Nanoparticulate TiO_2. *J. Phys. Chem. B* **2000**, *104*, 3624−3629.
(37) Rochford, J.; Chu, D.; Hagfeldt, A.; Galoppini, E. Tetrachelate Porphyrin Chromophores for Metal Oxide Semiconductor Sensitization: Effect of the Spacer Length and Anchoring Group Position. *J. Am. Chem. Soc.* **2007**, *129*, 4655−4665.
(38) Lee, C. Y.; She, C.; Jeong, N. C.; Hupp, J. T. Porphyrin Sensitized Solar Cells: TiO_2 Sensitization with a π-Extended Porphyrin Possessing Two Anchoring Groups. *Chem. Commun.* **2010**, *46*, 6090−6092.
(39) Hart, A. S.; KC, C. B.; Gobeze, H. B.; Sequeria, L. R.; D'Souza, F. Porphyrin-Sensitized Solar Cells. Effect of Carboxy Anchor Group Orientation on the Cell Performance. *ACS Appl. Mater. Interfaces* **2013**, *5*, 5314−5323.
(40) Kira, A.; Tanaka, M.; Umeyama, T.; Matano, Y.; Yoshimoto, N.; Zhang, Y.; Ye, S.; Lehtivuori, H.; Tkachenko, N. V.; Lemmetyinen, H.; Imahori, H. Hydrogen Bonding Effects on Film Structure and Photoelectrochemical Properties of Nanostructured TiO_2 Electrodes Modified with Porphyrin and Fullerene Composites. *J. Phys. Chem. C* **2007**, *111*, 13618−13626.
(41) Imahori, H.; Hayashi, S.; Hayashi, H.; Oguro, A.; Eu, S.; Umeyama, T.; Matano, Y. Effects of Porphyrin Substituents and Adsorption Conditions on Photovoltaic Properties of Porphyrin-Sensitized TiO_2 Cells. *J. Phys. Chem. C* **2009**, *113*, 18406−18413.
(42) Eu, S.; Hayashi, S.; Umeyama, T.; Oguro, A.; Kawasaki, M.; Kadota, N.; Matano, Y.; Imahori, H. Effects of 5-Membered Heteroaromatic Spacers on Structures of Porphyrin Films and Photovoltaic Properties of Porphyrin-Sensitized TiO_2 Cells. *J. Phys. Chem. C* **2007**, *111*, 3528−3537.
(43) Tanaka, M.; Hayashi, S.; Eu, S.; Umeyama, T.; Matano, Y.; Imahori, H. Novel Unsymmetrical π-Elongated Porphyrins for Dye-Sensitized Solar Cells. *Chem. Commun.* **2007**, 2069−2071.
(44) Hayashi, S.; Matsubara, Y.; Eu, S.; Hayashi, H.; Umeyama, T.; Matano, Y.; Imahori, H. Fused Five-Membered Porphyrin for Dye-Sensitized Solar Cells. *Chem. Lett.* **2008**, *37*, 846−847.
(45) Eu, S.; Hayashi, S.; Umeyama, T.; Matano, Y.; Araki, Y.; Imahori, H. Carboxyquinoxaline-Fused Porphyrins for Dye-Sensitized Solar Cells. *J. Phys. Chem. C* **2008**, *112*, 4396−4405.
(46) Hayashi, S.; Tanaka, M.; Hayashi, H.; Eu, S.; Umeyama, T.; Matano, Y.; Araki, Y.; Imahori, H. Naphthyl-Fused π-Elongated Porphyrins for Dye-Sensitized TiO_2 Cells. *J. Phys. Chem. C* **2008**, *112*, 15576−15585.
(47) Imahori, H.; Matsubara, Y.; Iijima, H.; Umeyama, T.; Matano, Y.; Ito, S.; Niemi, M.; Tkachenko, N. V.; Lemmetyinen, H. Effects of meso-Diarylamino Group of Porphyrins as Sensitizers in Dye-Sensitized Solar Cells on Optical, Electrochemical, and Photovoltaic Properties. *J. Phys. Chem. C* **2010**, *114*, 10656−10666.
(48) Kira, A.; Matsubara, Y.; Iijima, H.; Umeyama, T.; Matano, Y.; Ito, S.; Niemi, M.; Tkachenko, N. V.; Lemmetyinen, H.; Imahori, H. Effects of π-Elongation and Fused Position of Quinoxaline-Fused Porphyrins as Sensitizers in Dye-Sensitized Solar Cells on Optical, Electrochemical, and Photovoltaic Properties. *J. Phys. Chem. C* **2010**, *114*, 11293−11304.
(49) Imahori, H.; Iijima, H.; Hayashi, H.; Toude, Y.; Umeyama, T.; Matano, Y.; Ito, S. Bisquinoxaline-Fused Porphyrins for Dye-Sensitized Solar Cells. *ChemSusChem* **2011**, *4*, 797−805.
(50) Mathew, S.; Iijima, H.; Toude, Y.; Umeyama, T.; Matano, Y.; Ito, S.; Tkachenko, N. V.; Lemmetyinen, H.; Imahori, H. Optical, Electrochemical, and Photovoltaic Effects of an Electron-Withdrawing Tetrafluorophenylene Bridge in a Push-Pull Porphyrin Sensitizer used for Dye-Sensitized Solar Cells. *J. Phys. Chem. C* **2011**, *115*, 14415−14424.
(51) Hayashi, H.; Touchy, A. S.; Kinjo, Y.; Toude, Y.; Kurotobi, K.; Umeyama, T.; Matano, Y.; Imahori, H. Triarylamine-Substituted Imidazole- and Quinoxaline-Fused Push-Pull Porphyrin for High Performance Dye-Sensitized Solar Cell. *ChemSusChem* **2013**, *6*, 508−517.
(52) Kurotobi, K.; Kawamoto, K.; Toude, Y.; Fujimori, Y.; Kinjo, Y.; Ito, S.; Matano, Y.; Imahori, H. Synthesis and Photovoltaic Properties of Phenylethynyl-Substituted Diazaporphyrin. *Chem. Lett.* **2013**, *42*, 725−726.
(53) Kurotobi, K.; Toude, Y.; Kawamoto, K.; Fujimori, Y.; Ito, S.; Chabera, P.; Sundström, V.; Imahori, H. Highly Asymmetrical Porphyrins with Enhanced Push-Pull Character for Dye-Sensitized Solar Cells. *Chem. - Eur. J.* **2013**, *19*, 17075−17081.
(54) Lee, C.-W.; Lu, H.-P.; Lan, C.-M.; Huang, Y.-L.; Liang, Y.-R.; Yen, W.-N.; Liu, Y.-C.; Lin, Y.-S.; Diau, E. W.-G.; Yeh, C.-Y. Novel Zinc Porphyrin Sensitizers for Dye-Sensitized Solar Cells: Synthesis and Spectral, Electrochemical, and Photovoltaic Properties. *Chem. - Eur. J.* **2009**, *15*, 1403−1412.
(55) Lu, H.-P.; Mai, C.-L.; Tsia, C.-Y.; Hsu, S.-J.; Hsieh, C.-P.; Chiu, C.-L.; Yeh, C.-Y.; Diau, E. W.-G. Design and Characterization of Highly Efficient Porphyrin Sensitizers for Green See-Through Dye-Sensitized Solar Cells. *Phys. Chem. Chem. Phys.* **2009**, *11*, 10270−10274.
(56) Lin, C.-Y.; Wang, Y.-C.; Hsu, S.-J.; Lo, C.-F.; Diau, E. W.-G. Preparation and Spectral, Electrochemical, and Photovoltaic Properties of Acene-Modified Zinc Porphyrins. *J. Phys. Chem. C* **2010**, *114*, 687−693.

DOI: 10.1021/acsami.5b05163
ACS Appl. Mater. Interfaces 2015, 7, 18689−18696

(57) Hsieh, C.-P.; Lu, H.-P.; Chiu, C.-L.; Lee, C.-W.; Chung, S.-H.; Mai, C.-L.; Yen, W.-N.; Hsu, S.-J.; Diau, E. W.-G.; Yeh, C.-Y. Synthesis and Characterization of Porphyrin Sensitizers with Various Electron-Donating Substituents for Highly Efficient Dye-Sensitized Solar Cells. *J. Mater. Chem.* **2010**, *20*, 1127−1134.
(58) Wu, S.-L.; Lu, H.-P.; Yu, H.-T.; Chuang, S.-H.; Chiu, C.-L.; Lee, C.-W.; Diau, E. W.-G.; Yeh, C.-Y. Design and Characterization of Porphyrin Sensitizers with a Push-Pull Framework for Highly Efficient Dye-Sensitized Solar Cells. *Energy Environ. Sci.* **2010**, *3*, 949−955.
(59) Bessho, T.; Zakeeruddin, S. M.; Yeh, C.-Y.; Diau, E. W.-G.; Grätzel, M. Highly Efficient Mesoscopic Dye-Sensitized Solar Cells Based on Donor−Acceptor-Substituted Porphyrins. *Angew. Chem., Int. Ed.* **2010**, *49*, 6646−6649.
(60) Yella, A.; Lee, H.-W.; Tsao, H. N.; Yi, C.; Chandiran, A. K.; Nazeeruddin, S. M.; Diau, E. W.-G.; Yeh, C.-Y.; Zakeeruddin, S. M.; Grätzel, M. Porphyrin-Sensitized Solar Cells with Cobalt (II/III)−Based Redox Electrolyte Exceed 12% Efficiency. *Science* **2011**, *334*, 629−634.
(61) Lu, J.; Xu, X.; Cao, K.; Cui, J.; Zhang, Y.; Shen, Y.; Shi, X.; Liao, L.; Cheng, Y.; Wang, M. D-π-A Structured Porphyrins for Efficient Dye-Sensitized Solar Cells. *J. Mater. Chem. A* **2013**, *1*, 10008−10015.
(62) Luo, J.; Xu, M.; Li, R.; Huang, K.-W.; Jiang, C.; Qi, Q.; Zeng, W.; Zhang, J.; Chi, C.; Wang, P.; Wu, J. N-Annulated Perylene as An Efficient Electron Donor for Porphyrin-Based Dyes: Enhanced Light-Harvesting Ability and High-Efficiency Co(II/III)-Based Dye-Sensitized Solar Cells. *J. Am. Chem. Soc.* **2014**, *136*, 265−272.
(63) Wu, C.-H.; Chen, M.-C.; Su, P.-C.; Kuo, H.-H.; Wang, C.-L.; Lu, C.-Y.; Tsai, C.-H.; Wu, C.-C.; Lin, C.-Y. Porphyrins for Efficient Dye-Sensitized Solar Cells Covering the Near-IR Region. *J. Mater. Chem. A* **2014**, *2*, 991−999.
(64) Yella, A.; Mai, C.-L.; Zakeeruddin, S. M.; Chang, S.-N.; Hsieh, C.-H.; Yeh, C.-Y.; Grätzel, M. Molecular Engineering of Push−Pull Porphyrin Dyes for Highly Efficient Dye-Sensitized Solar Cells: The Role of Benzene Spacers. *Angew. Chem., Int. Ed.* **2014**, *53*, 2973−2977.
(65) Mathew, S.; Yella, A.; Gao, P.; Humphry-Baker, R.; Curchod, B. F. E.; Ashari-Astani, N.; Tavernelli, I.; Rothlisberger, U.; Nazeeruddin, M. K.; Grätzel, M. Dye-Sensitized Solar Cells with 13% Efficiency Achieved Through the Molecular Engineering of Porphyrin Sensitizers. *Nat. Chem.* **2014**, *6*, 242−247.
(66) Imahori, H.; Kang, S.; Hayashi, H.; Haruta, M.; Kurata, H.; Isoda, S.; Canton, S. E.; Infahsaeng, Y.; Kathiravan, A.; Pascher, T.; Chábera, P.; Yartsev, A. P.; Sundström, V. Photoinduced Charge Carrier Dynamics of Zn-Porphyrin-TiO_2 Electrodes − the Key Role of Charge Recombination for Solar Cell Performance. *J. Phys. Chem. A* **2011**, *115*, 3679−3690.
(67) Ye, S.; Kathiravan, A.; Hayashi, H.; Tong, Y.; Infahsaeng, Y.; Chabera, P.; Pascher, T.; Yartsev, A. P.; Isoda, S.; Imahori, H.; Sundström, V. Role of Binding Structures of Zn-Porphyrin on TiO_2 in Dye-Sensitized Solar Cells Studied by Sum Frequency Generation (SFG) Vibrational Spectroscopy and Ultrafast Spectroscopy. *J. Phys. Chem. C* **2013**, *117*, 6066−6080.
(68) Bittner, A. M.; Epple, M.; Kuhnke, K.; Houriet, R.; Heusler, A.; Vogel, H.; Seitsonen, A. P.; Kern, K. Conformations of an Amino-Amido-Thiolate Self-Assembled Layer on Gold in Air and in Electrolytes. *J. Electroanal. Chem.* **2003**, *550-551*, 113−124.
(69) De Cat, I.; Guo, Z.; George, S. J.; Meijer, E. W.; Schenning, A. P. H. J.; De Feyter, S. Induction of Chirality in an Achiral Monolayer at the Liquid/Solid Interface by a Supramolecular Chiral Auxiliary. *J. Am. Chem. Soc.* **2012**, *134*, 3171−3177.
(70) Terada, K.; Kanaizuka, K.; Iyer, V. M.; Sannodo, M.; Saito, S.; Kobayashi, K.; Haga, M. Memory Effects in Molecular Films of Free-Standing Rod-Shaped Ruthenium Complexes on an Electrode. *Angew. Chem., Int. Ed.* **2011**, *50*, 6287−6291.

DOI: 10.1021/acsami.5b05163
ACS Appl. Mater. Interfaces 2015, 7, 18689−18696